TEMPORARY OVERVOLTAGES IN POWER SYSTEMS

Juan A. Martinez-Velasco
Universitat Politècnica de Catalunya, Barcelona, Spain

Francisco González-Molina
Universitat Rovira i Virgili, Tarragona, Spain

Keywords: Ground fault overvoltages, ferro-resonance, harmonics, inrush currents, load rejection, power systems, modeling, resonance, transformer energization, transient analysis.

Contents

Summary

Temporary overvoltages (TOVs) are undamped or little damped power-frequency overvoltages of relatively long duration (i.e., seconds, even minutes). These overvoltages are typically caused by faults to ground, resonance conditions, load rejection, energization of unloaded transformers, or a combination of these. Resonance is a synchronization between a natural oscillation of the power system and the frequency of an external sinusoidal source. This phenomenon leads to increased voltages and/or currents. A variation can be found in what is called ferro-resonance. This term applies to a wide variety of interactions between capacitors and iron-core magnetizing inductances that again can result in high overvoltages and cause failures in transformers, cables, and arresters. On the other hand, the load rejection phenomenon is a sudden three-pole switching event of a system with three similar phase-to ground voltage rises, resulting in the same relative overvoltages phase-to-ground and phase-to-phase. Resonance overvoltages may appear also when a line and a transformer are energized together. Re-energizing a transformer can cause high inrush currents due to the nonlinear behavior of its core. Those currents can have a high magnitude with a significant harmonic content.

(TOVs) can be classified according to their frequency of oscillation, being higher, equal or lower than the power frequency. The chapter is structured basically in two parts: modeling guidelines that can be applied for calculating TOVs, with special mention to the required power-frequency models (power sources, lines and cables, transformers, loads, etc) for the transient analysis; and description, in detail, of the analysis and simulation of the most common types of TOVs.

1. Introduction

TOVs are undamped or weakly damped oscillatory phase-to-ground, phase-to-phase or longitudinal voltage stresses of relatively long duration (i.e., seconds, even minutes). They are often preceded by a transient overvoltage resulting from a switching operation, and caused under operating conditions with very little damping, a condition that can be often associated with light load or no load at all. It can also be assumed that there is either a source of voltage driving the system at an elevated level or some mechanism that is counteracting the damping (IEC 60071-1, 2010; IEC 60071-2, 1996; IEEE Std C62.82.1, 2010; IEEE Std 1313.2, 1999; Glavitsch, 1980).

TOVs are characterized by their amplitudes, their voltage shape and their duration. All parameters depend on the origin of the overvoltages, and amplitudes and shapes may even vary during the overvoltage duration (IEC 60071-1, 2010; IEEE Std C62.82.1, 2010). They can also be characterized by their oscillating frequency (Glavitsch, 1980).

The representative TOV is characterized by a standard short duration (1 min) power-frequency waveshape (IEC 60071-1, 2010; IEEE Std C62.82.1, 2010).

The form, frequency and ways of initiation of TOVs offer various possibilities for their classification. TOVs can be classified upon their origin, by the mechanism by which they are sustained, or by their oscillating frequency, which may be equal, higher or lower than the natural power frequency of the system.

The most frequent causes of TOVs are faults to ground, load rejection, resonance and ferro-resonance. Except for some types of resonances and for ferro-resonance, these causes are also associated to slow-front overvoltages. For instance, a phase-to-ground fault can cause a slow-front overvoltage during fault initiation and clearing, and a TOV when the during-fault steady-state condition is reached.

A summary of the main causes that lead to TOVs is presented below.

Faults to ground: Phase-to-ground faults may produce power frequency phase-to-ground overvoltages on the unfaulted phases. TOVs between phases or across longitudinal insulation normally do not arise (IEC 60071-2, 1996). The overvoltage magnitude depends on the system grounding and on the fault location. The duration of the overvoltage corresponds to the duration of the fault (until fault clearing). In effectively grounded systems, the TOV is about 1.3 pu and the duration of the overvoltage, including fault clearing, is generally less than 1 s. In resonant grounded systems the TOV is about 1.73 pu or greater and, with fault clearing, the duration is generally less than 10 s. Depending on the system configuration, separated portions of the system may become ungrounded during fault clearing, and high overvoltages can be produced in the separated part.

Load rejection: Overvoltages may arise when a loaded system becomes suddenly unloaded. Phase-to-ground and longitudinal TOVs caused by load rejection are a function of the rejected load, the system topology after disconnection, and the characteristics of the sources (e.g., speed and voltage regulators of generators). In a symmetrical three-phase power system the same relative overvoltages occur phase-to-ground and phase-to-phase. The longitudinal TOVs depend on whether phase angle difference is possible, the worst possible situation being a phase opposition; such situation can occur when the voltages on each side of the open switching device are not synchronized. A distinction should be made between various system configurations when large loads are rejected. The rises may be especially important in the case of load rejection at the remote end of a long line (Ferranti effect) and they mainly affect the apparatus at the station connected on the source side of the remote open circuit-breaker. A system with relatively short lines and high short circuit power at terminal stations will have low overvoltages, whereas a system with long lines and low short circuit power at generating sites (which are usual in the extra-high voltage range at their initial stage) will have high overvoltages.

Resonance and ferro-resonance: TOVs may arise from the interaction of capacitive elements (lines, cables, series capacitors) and inductive elements (transformers, shunt reactors). The resonant overvoltage is initiated by a sudden change in the system

configuration (e.g., load rejection, single-phase switching of a transformer terminated line, isolation of a bus potential transformer through breaker capacitance, connection of a capacitor bank). Resonant and ferro-resonant overvoltages can have magnitudes greater than 3.0 pu and last until the condition is cleared or a power component is damaged.

Transformer energization: Resonance overvoltages can occur when a line and an unloaded or lightly loaded transformer are energized together. The transformer can cause inrush currents due to the nonlinear behavior of its core. The inrush currents, which can have a high magnitude with a significant harmonic content, will interact with the power system, whose frequency response may exhibit a resonance at a frequency included in the transformer inrush current. The consequence may be a long-duration resonant TOV (Durbak, 2006).

Combinations of temporary overvoltage origins: The combination of TOVs of different origin may lead to higher arrester ratings and consequently to higher protection and insulation levels. The combination *ground fault with load rejection* is an example that can occur when, during a fault on the line, the load side breaker opens first and the disconnected load causes a load rejection overvoltage in the faulted part of the system before the supply side circuit-breaker opens (IEC 60071-2, 1996). This combination can also exist when a large load is switched off and the subsequent TOV causes a ground fault on the remaining system. The probability of such an event, however, is small, when the overvoltages due to the change of load are themselves small and a subsequent fault is only likely to occur in extreme conditions; e.g., under heavy pollution. The combination can further occur as a result of a line fault followed by failure of a circuit-breaker to open. The probability of such a combination, although small, is not negligible since these events are not statistically independent. Such an occurrence, which results from a generator connected through a transformer to a faulted long line, can result in a significant slow-front transient overvoltage on the healthy phase and a prolonged variable TOV which is a function of generator characteristics and governor-voltage regulator actions. When the probability of such combinations is assumed high, system studies are recommended. The combination of resonance phenomena with other origins should only be considered as an additional result of these resonances, since these phenomena must be avoided. When resonance phenomena cannot be avoided, it is also recommendable to carry out detailed studies.

Longitudinal overvoltages may occur during *synchronization* due to phase opposition at both sides of the switch. The representative longitudinal TOVs are derived from the expected overvoltage, which has amplitude equal to twice the phase-to-ground operating voltage and duration of several seconds to some minutes. When synchronization is frequent, the probability of occurrence of a ground fault and consequent overvoltage shall be considered; in such cases the representative overvoltage amplitudes are the sum of the assumed maximum ground-fault overvoltage on one terminal and the continuous operating voltage in phase opposition on the other (IEC 60071-2, 1996).

A classification based on the frequency of oscillation distinguishes three classes of TOVs (Glavitsch, 1980).

- *Overvoltages with a frequency of oscillation equal to the power frequency*: This group includes overvoltages at or near the power frequency being the waveshape either a pure sinusoid or with a low harmonic content/distortion. The voltage shape will usually exhibit a slowly decaying. This type of overvoltage is usually preceded by a transient overvoltage immediately after the causing event; e.g. a switching operation. Overvoltages caused after line energization, as well as overvoltages arising under linear conditions, belong to this group.
- *Overvoltages with a frequency of oscillation higher than the power frequency*: In general, they are due to nonlinearities, which can result from power electronics, saturated magnetic characteristics of transformers, shunt reactors, and measurement transformers. Although these overvoltages are always a superposition of harmonics and the fundamental, the harmonic component is dominant. TOVs of this type may also be preceded by transients or some other abnormal state.
- *Overvoltages with a frequency of oscillation lower than the power frequency*: They are either true sub-harmonic voltages or voltages of a frequency below the power frequency. These overvoltages usually appear across series capacitors. Often it is not the voltage itself which is a nuisance, but the sub-harmonic or low-frequency current.

For a more extended list of TOVs, their causes and characterization, see (German & Haddad, 2004).

The analytical means for the assessment of TOVs can be categorized according to the type and origin. Power-frequency overvoltages originating from a weak supply and insufficient reactive compensation can be most easily analyzed by linear models, but the analysis of systems with harmonics of all sorts requires nonlinear and iterative techniques. Several means for the reduction or mitigation of TOVs have been developed because their origin is not unique. The list of methods includes damping measures, reactive compensation, and the use of surge arresters.

TOVs are used to select surge arresters; that is, arresters are selected to withstand these overvoltages, which are not usually limited by surge arresters. The TOV level has become a determining parameter for selecting the rated voltage of arresters and thus the permanent overvoltage level of the material in general. Resonant and ferro-resonant overvoltages are an exception and they should not be used for arrester selection, instead they should be limited by detuning the system from the resonant frequency, by changing the system configuration, or by installing damping resistors. The following section summarizes the modeling guidelines that can be applied for calculating TOVs. The main sections of the chapter are dedicated to the analysis and simulation of the most common types of TOVs, although a special attention is paid to the phenomenon of ferro-resonance.

2. Modeling Guidelines for Analysis of Temporary Overvoltages

TOVs arise with frequencies close to the power frequency, usually below 1 kHz, so the models required for their analysis are power-frequency models for which the frequency dependence of parameters is not usually a concern.

A methodology for analysis of TOVs is presented in IEC TR 60071-4 (2004), which provides guidelines for representing components and for determining the study zone, and a discussion about the required input data. The IEC report does not cover ferro-resonance.

A summary of the guidelines proposed in the literature is presented below; for more details see CIGRE WG 33.02 (1990), Gole, Martinez-Velasco, & Keri (1998), and IEC TR 60071-4 (2004).

- The power supply model will depend on the case study. It can be represented as an ideal voltage source in series with a three-phase impedance (specified by its positive- and zero-sequence impedances), as a synchronous generator, or as a network equivalent whose impedance has been fitted in a frequency range typically below 1 kHz. If a synchronous generator model is required, then it can be represented by the generalized Park's model with complete models of the electrical and mechanical parts, including saturation, and control units. Since the dynamic behavior of generators does not significantly influence TOVs, an alternative option is to represent generators by a sine wave source behind their subtransient reactance, with phases of voltage sources determined from load-flow results.
- Lines and cables can be described either by a distributed line model with frequency-dependent parameters, fitted within a range of a few kHz, or by a lumped-parameter frequency-independent pi model. A lumped-parameter model can be accurate enough for TOV analysis, because the positive sequence resistance and inductance do not significantly vary below 1 kHz (CIGRE WG 33.02, 1990), which covers the frequency range of phenomena related to most TOVs. Lines and cables can be represented by a pi-equivalent with parameters calculated at power frequency, although in some cases zero-sequence parameters must be fitted in a frequency range of up 1 kHz. The number of pi-sections required for representing a line/cable will depend on the length and the frequency range of the phenomena to be analyzed; a rule is to consider one pi-cell per harmonic multiple of the fundamental. Line transpositions and cable cross-bonding will also affect the number of pi-sections.
- Corona effect is required only when the overvoltage can exceed the ionization threshold.
- Models of line towers and insulators are not required, although footing impedance models may be required in some fault calculations; in such case a low-frequency low-current model will suffice.
- Models for transformers, shunt reactors and capacitor banks will be usually required. Transformer models should be implemented with caution, mainly in ferro-resonant studies. For most TOV studies, the transformer model must include the winding resistances, the leakage inductances, as well as the magnetizing characteristics of the core. To account for remnant fluxes in the iron core, hysteresis has to be included in the model. The remnant fluxes in the transformer core can be obtained via the integration of the voltages measured on the transformer windings during its disconnection. In ferro-resonance studies, the most critical part is the model of the transformer core and its saturation characteristics. Take into account that a saturable reactance can be a source of harmonics which may cause resonance problems.

- Models for loads and power electronic converters can be also required. As a rule of thumb a no load condition will usually represent the most conservative scenario, since load adds damping. However, in some cases a load model may be required to limit the conditions under which overvoltages can arise. Different approaches for representing loads were presented in IEC TR 60071-4 (2004). Loads and shunt devices, such as capacitors and reactors, can be modeled as constant impedances, calculated at power frequency. Models of power electronic converters are usually required mainly when the converter can be the source of harmonics that can cause resonance overvoltages. In such cases, including filter models is mandatory.
- Circuit breakers in a time-domain simulation of TOVs are mostly needed to control the closing time. They can be represented as ideal switches.
- Substation busbars models are not required since it can be assumed that the voltage is the same in the whole substation. However, some substation equipment and the substation ground grid may be required. For instance, the model of a voltage transformer can be critical in some ferro-resonance studies.

TOVs are used to select arresters, and the arrester model is not usually required. However, there are some exceptions for which the arrester model can be important; for instance, in the study of ferro-resonant overvoltages when arresters are installed.

3. Faults to Ground

3.1. Introduction

The magnitude of overvoltages due to ground faults depend on the method of system grounding (i.e., solidly grounded, resistance grounded, high resistance grounded or ungrounded systems), the equivalent sequence impedances see from the fault location, and the fault impedance. Their duration depend on the fault clearance times, and therefore, on the design of the protection system. An estimation of the duration and magnitude of these overvoltages is crucial for selection of surge arresters in most power systems.
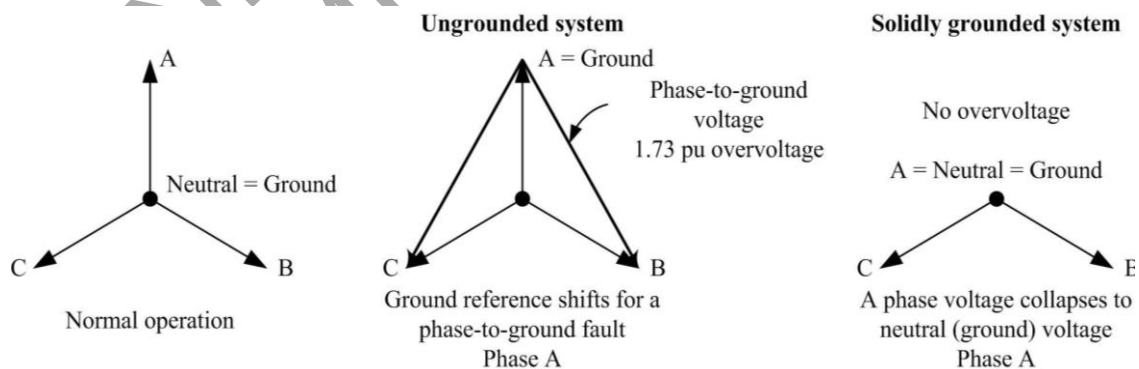
Figure 1. Voltage shifts as a function of the grounding configuration.

The system grounding configuration determines the overvoltages that can occur during a fault to ground. A single phase-to-ground fault shifts the ground potential at the fault location, depending on the severity of this shift on the grounding configuration (see

Figure 1). On a solidly grounded system with a good return path to the grounding source, the shift is usually negligible. On an ungrounded system, a full offset may occur and the phase-to-ground voltage on the unfaulted phases approaches the phase-to-phase voltage. On a multi-grounded distribution system with a solidly grounded station transformer, overvoltages above 1.3 pu are rare (EPRI Report, 2005).

3.2. Calculation of Ground Fault Overvoltages

The single phase-to-ground fault is the most important cause of TOVs in power systems, since in most system configurations this type of fault produces the maximum fault voltages.

Two factors may be used to measure this type of overvoltage (EPRI Report, 2005; Hileman, 1999; IEEE Std C62.22, 1997; IEC Std 60099-5, 2000):

- Coefficient of grounding (COG)

$$\text{COG} = \frac{V'_{\text{LN}}}{V_{\text{LL}}} \tag{1}$$

- Earth fault factor (EFF)

$$\text{EFF} = \frac{V'_{\text{LN}}}{V_{\text{LN}}} \tag{2}$$

where V'_{LN} is the maximum phase-to-ground voltage on the unfaulted phases during a fault, and V_{LN}, V_{LL} are respectively the nominal phase-to-neutral and phase-to-phase voltages.

Obviously:

$$\text{EFF} = \sqrt{3} \cdot \text{COG} \tag{3}$$

Consider the diagram shown in Figure 2. The equivalent circuit from the fault location is reduced to a three-phase symmetrical voltage source in series with the sequence impedances seen from this location.
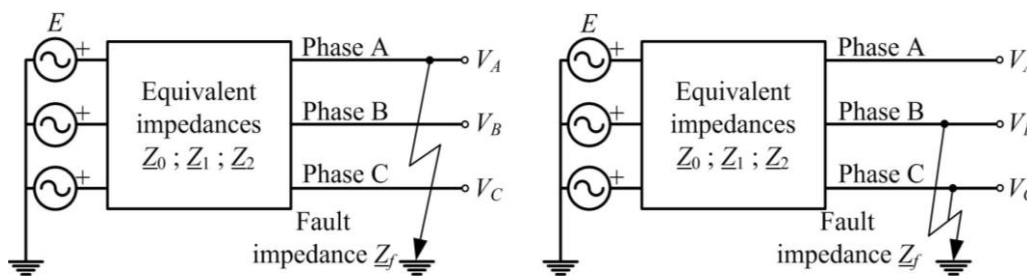
Figure 2. Equivalent circuit for calculation of ground fault overvoltages.

For a single phase-to-ground fault on phase A, the voltages on the unfaulted phases are (Das, 2002; Das, 2010):

$$\underline{V}_B^F = \frac{3\underline{a}^2\underline{Z}_f - j\sqrt{3}\cdot\left(\underline{Z}_2 - \underline{a}\underline{Z}_0\right)}{\underline{Z}_1 + \underline{Z}_2 + \underline{Z}_0 + 3\underline{Z}_f}\cdot\underline{E} \qquad (4a)$$

$$\underline{V}_C^F = \frac{3\underline{a}\underline{Z}_f + j\sqrt{3}\cdot\left(\underline{Z}_2 - \underline{a}^2\underline{Z}_0\right)}{\underline{Z}_1 + \underline{Z}_2 + \underline{Z}_0 + 3\underline{Z}_f}\cdot\underline{E} \qquad (4b)$$

where $\underline{a} = 1\angle120°$. $\underline{Z}_1$, $\underline{Z}_2$ and $\underline{Z}_0$ are respectively the positive-, negative- and zero-sequence impedances seen from the fault location. $\underline{Z}_f$ is the fault impedance and E is the phase-to-neutral voltage magnitude prior to the fault.

From the above results it follows that for $\underline{Z}_0 = 0$, the voltages of the unfaulted phases have the same magnitude, and when $\underline{Z}_0 \to \infty$, the magnitude of both voltages tends to the phase-to-phase voltage. Very high voltages occur when the difference between the phase angles of $\underline{Z}_1$ and $\underline{Z}_0$ is greater than 90°. In practice, this is only possible in power systems with isolated neutral, and because the zero sequence impedance is capacitive, whereas the positive and negative sequence impedances have an inductive character.

When $\underline{Z}_1 = \underline{Z}_2$, the voltages at the unfaulted phases are (EPRI Report, 2005; Das, 2002; Das, 2010):

$$\underline{V}_B^F = \left(\underline{a}^2 + \frac{\underline{Z}_1 - \underline{Z}_0}{2\underline{Z}_1 + \underline{Z}_0 + 3\underline{Z}_f}\right)\cdot\underline{E} \qquad (5a)$$

$$\underline{V}_C^F = \left(\underline{a} + \frac{\underline{Z}_1 - \underline{Z}_0}{2\underline{Z}_1 + \underline{Z}_0 + 3\underline{Z}_f}\right)\cdot\underline{E} \qquad (5b)$$

For a double phase-to-ground fault on phases B and C, the voltage on the unfaulted phase is:

$$\underline{V}_A^F = \left(\frac{3\underline{Z}_0 + 6\underline{Z}_f}{\underline{Z}_1 + 2\underline{Z}_0 + 6\underline{Z}_f}\right)\cdot\underline{E} \qquad (6)$$

In some special cases, the double phase-to-ground fault causes overvoltages that are slightly higher than the single phase-to-ground fault. But because single phase-to-ground faults are so much more common, the analysis is based on these faults, for which the resulting voltage on the unfaulted phases is always higher when the fault impedance is zero, which may not be always the case for double phase-to-ground faults. A system is *effectively grounded* if the coefficient of grounding is less than or equal to 80% (so the earth fault factor is less than 138%) (EPRI Report, 2005). This situation is met approximately when $X_0 / X_1 < 3$ and $R_0 / X_1 < 3$.

Solidly grounded systems (i.e., systems where no intentional impedance is introduced between system neutral and ground) generally meet the definition of effectively grounded, since the ratio X_0/X_1 is positive and less than 3.0 and the ratio R_0/X_0 is positive and less than 1.0, where X_1, X_0, and R_0 are the positive sequence reactance, zero sequence reactance, and zero sequence resistance, respectively. These systems are, generally, characterized by a COG of about 0.8.

It is difficult to assign X_0/X_1 and R_0/X_0 values for ungrounded systems (i.e., systems with no intentional connection to ground except through potential transformers, metering devices of high impedance or distributed phase capacitances), since the ratio X_0/X_1 is negative and may vary from low to high values. The COG may approach 1.2 pu. For values of X_0/X_1 between 0 and –40, the possibility of resonance with consequent generation of high voltages exists.

Table 1 provides some typical values of the coefficient of grounding for different grounding systems (Hileman, 1999; IEEE Std C62.22, 1997; IEC Std 60099-5, 2000).

System grounding	COG (pu)
Grounded systems	
• High short-circuit capacity	0.69 to 0.80
• Low short-circuit capacity	0.69 to 0.87
• Low impedance	0.80 to 1.0
Resonant grounded systems	
• Meshed network	1.0
• Radial lines	1.0 to 1.15
Isolated systems	
• Distribution	1.0 to 1.04

Table 1. Typical values for the Coefficient of Grounding – Faults to Ground

The COG can be calculated by the equations described below (Das, 2002; Das, 2010):
  • Single phase-to-ground fault:

$$\text{Phase B}\quad \text{COG} = \left| -\frac{1}{2}\left(\frac{\sqrt{3}\underline{k}}{2+\underline{k}} + j1 \right) \right| \tag{7a}$$

$$\text{Phase C}\quad \text{COG} = \left| -\frac{1}{2}\left(\frac{\sqrt{3}\underline{k}}{2+\underline{k}} - j1 \right) \right| \tag{7b}$$

  • Double phase-to-ground fault:

$$\text{Phase A}\quad \text{COG} = \left| \frac{\sqrt{3}\underline{k}}{1+2\underline{k}} \right| \tag{8}$$

where $\underline{k}$ is given by:

$$\underline{k} = \frac{\underline{Z}_0}{\underline{Z}_1} \tag{9}$$

When the fault impedance is just a resistance, $\underline{k}$ can be modified as follows to take into account the fault resistance (Das, 2010):

$$\underline{k} = \frac{R_0 + R_f + jX_0}{R_1 + R_f + jX_1} \qquad \text{single phase-to-ground fault} \tag{10a}$$

$$\underline{k} = \frac{R_0 + 2R_f + jX_0}{R_1 + 2R_f + jX_1} \qquad \text{double phase-to-ground fault} \tag{10b}$$

If resistances are neglected, then the above equations reduce to:

$$COG = \frac{\sqrt{1+k+k^2}}{2+k} \qquad \text{single phase-to-ground fault} \tag{11a}$$

$$COG = \frac{\sqrt{3}k}{1+2k} \qquad \text{double phase-to-ground fault} \tag{11b}$$

where

$$k = \frac{X_0}{X_1} \tag{12}$$

Figure 3 shows the EFF as a function of sequence impedances, namely the ratios R_1/X_1, X_0/X_1 and R_0/X_1 assuming that $X_1 = X_2$ (IEC 60071-2, 1996); see also (EPRI Report, 2005). The numbers on the curves indicate the EFF for the area bonded by the curve and the axes. All impedances must be on the same MVA base.

In general, fault resistance will reduce EFF, except in low-resistance systems. In extended resonant-grounded networks, the earth fault factor may be higher at other locations than the fault. The range of high values for X_0/X_1 positive and/or negative, apply to resonant grounded or isolated neutral systems; low values of positive X_0/X_1 apply to grounded neutral systems, whereas low values of negative X_0/X_1 is not suitable for practical application due to resonant conditions (IEC 60071-2, 1996).
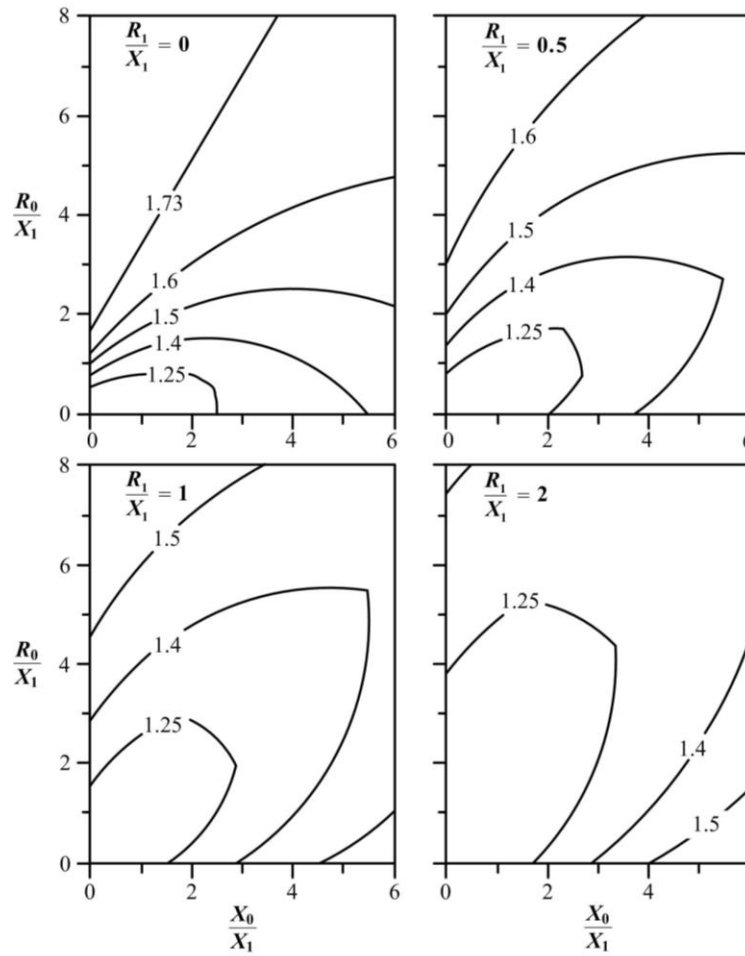
Figure 3. Earth fault factor in per unit for phase-to-ground faults (the contours mark the threshold of voltage).

3.3. Case Study

Figure 4 shows the diagram of the test system, in which a 110 kV subtransmission line is fed from a step-down transformer. The transformer is Y-Y connected being the neutral at the 220 kV side ungrounded, while the neutral at the 110 kV side will be connected to ground with a reactor of variable impedance. The subsequent plots depict the initial transient overvoltage and the TOVs that result when provoking both single-phase-to-ground and double-phase-to-ground faults at the sending end of the line with two different combinations of positive- and zero-sequence impedances. All simulation results were derived from the assumption of bolted fault; that is $\underline{Z}_f = 0$.
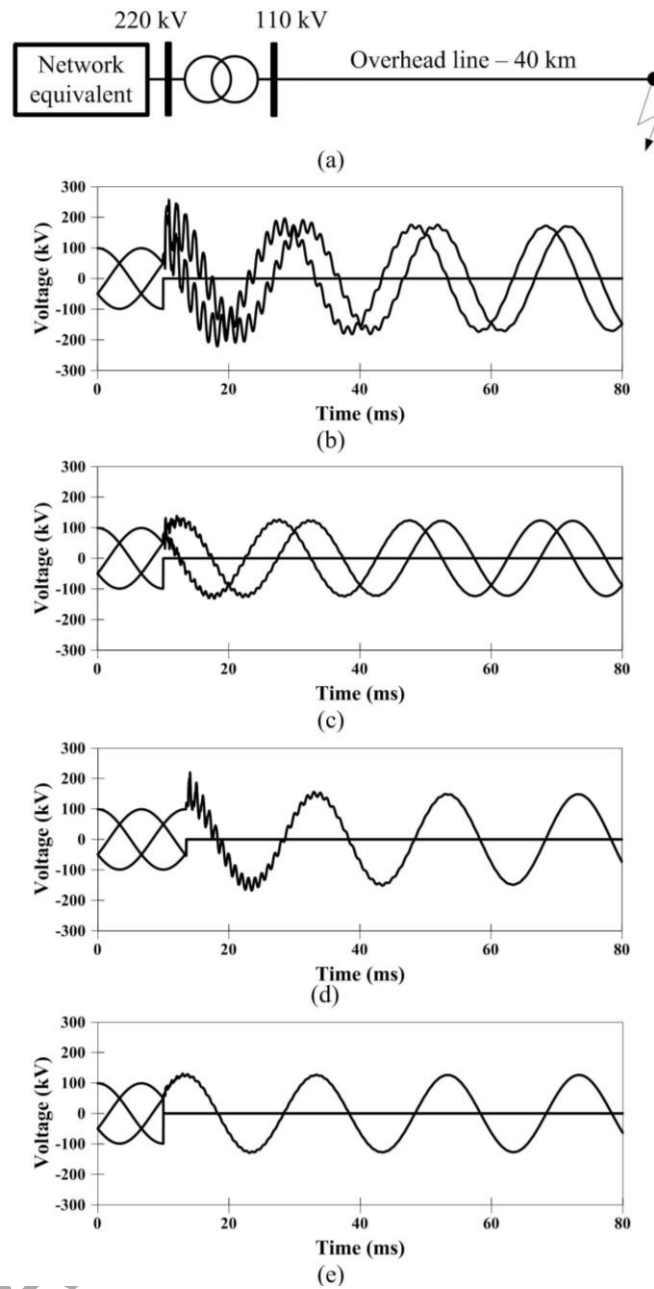
Figure 4: Fault overvoltage study. (a) Diagram of the test system. Simulation results: (b) Single-phase-to-ground fault – $\underline{Z}_1 = \underline{Z}_2 = 23.5\angle79°$, $\underline{Z}_0 = 20350\angle90°$, $\underline{Z}_f = 0$ Ω. (c) Double-phase-to-ground fault – $\underline{Z}_1 = \underline{Z}_2 = 23.5\angle79°$, $\underline{Z}_0 = 20350\angle90°$, $\underline{Z}_f = 0$ Ω. (d) Single-phase-to-ground fault – $\underline{Z}_1 = \underline{Z}_2 = 23.5\angle79°$, $\underline{Z}_0 = 68.5\angle80°$, $\underline{Z}_f = 0$ Ω. (e) Double-phase-to-ground fault – $\underline{Z}_1 = \underline{Z}_2 = 23.5\angle79°$, $\underline{Z}_0 = 68.5\angle80°$, $\underline{Z}_f = 0$ Ω.

From the formulas presented above the following coefficients are obtained:

- For $\underline{Z}_1 = \underline{Z}_2 = 23.5\angle79°$, $\underline{Z}_0 = 20350\angle90°$, $\underline{Z}_f = 0$ Ω

  $\underline{k} \approx 866\angle11°$, EFF for single-phase-to-ground fault ≈ 1.73, EFF for double-phase-to-ground fault ≈ 1.50

- For $\underline{Z}_1 = \underline{Z}_2 = 23.5\angle79°$, $\underline{Z}_0 = 68.5\angle80°$, $\underline{Z}_f = 0$ Ω

$\underline{k} \approx 2.91\angle1°$, EFF for single-phase-to-ground fault ≈ 1.24, EFF for double-phase-to-ground fault ≈ 1.28

Since the peak voltage in all phases prior to the fault is 99 kV, it is easy to check that the peak voltage of the resulting steady-state voltage in the unfaulted phases is in all cases very close to the voltage that results from using the above factors. Take into account that a value of 99 kV is about 10% above the rated peak voltage of a 110 kV system.

Observe that for an ungrounded system (i.e., a non-effectively grounded system), the peak voltage that results during the initial transient reaches very high values, namely about 2.5 pu in the case of single-phase-to-ground fault, and little more than 2 pu in the case of a double-phase-to-ground fault.

4. Load Rejection

4.1. Introduction

Load rejection is a sudden three-pole switching event of a system with three similar phase-to-ground voltage rises; therefore, the same relative overvoltages occur phase-to-ground and phase-to-phase, so phase-to-ground and longitudinal TOVs may occur after load rejection. The voltage rises depend on the rejected load; they may be especially important in the case of load rejection at the remote end of a long line due to Ferranti effect.

4.2. Calculation of Load Rejection Overvoltages

Power flow across an impedance causes a voltage difference between the sending and receiving ends when the load has an inductive component. If the load is suddenly disconnected, a power-frequency voltage increase may result at the point of load connection. Although an electromagnetic transient occurs and it causes voltage surges in the system, for voltage rise estimation the system can be simply modeled by reducing it to the power-frequency short-circuit impedance seen from the point of load connection.
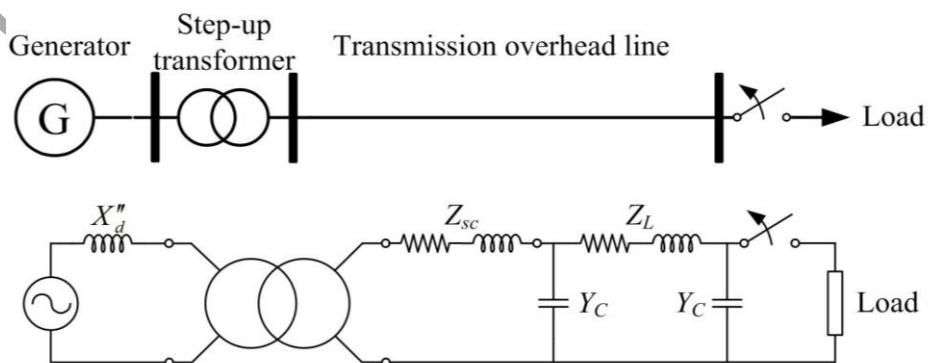
Figure 5. Diagram and equivalent circuit of the test system for load rejection analysis.

Consider the system depicted in Figure 5. It is a very general configuration for load rejection analysis that consists of a generator, a step-up transformer and a transmission line (although it may also be a cable). Note that the generator is represented by its internal emf behind its subtransient reactance, the transformer model includes its short-circuit impedance (in this case referred to its secondary side), and the line is represented by it pi-equivalent model with constant parameters calculated at power frequency. Assume that the transformation ratio of the transformer can be variable. The model is single-phase since the transient process is assumed symmetrical.

Under steady state conditions, the excitation of the generator and the regulation of the step-up transformer are controlled in such a way that the operating voltages do not exceed the highest permissible voltage of the system. Due to the loading, the internal voltage of the generator will be higher or much higher than 1 pu. After a sudden load shedding, an overexcited generator will remain supplying the transformer and the open circuited transmission line. This change of the system configuration can lead to a power-frequency TOV, which can be mitigated by the generator exciter within a few seconds.

The phenomena that occur after load rejection in the three main components may be summarized as follows.

Generator: The transient event can be approximated by using the equivalent circuit shown in Figure 5 in which the generator is represented by a constant voltage source behind its subtransient impedance. If the current change is assumed to be sudden, the subtransient voltage that appears in the shape of the terminal voltage depends on both the initial steady state and the subtransient reactance.

Without a voltage regulator, the terminal voltage of the generator rises, being the process governed by the no-load time constants. Since such a voltage stress may not be acceptable, a fast voltage regulation is needed. In the moment of load rejection the exciting voltage may even reverse, and after a few hundred milliseconds it is set to the no-load exciting voltage.

Transformer: The load current under normal operating conditions produces a voltage drop over the short circuit impedance of a transformer. This voltage drop can be compensated by the voltage regulator of the transformer. In any case, the secondary voltage will not exceed the maximum permissible voltage. However, after load rejection the secondary voltage goes up and may exceed the maximum voltage; that is, the magnitude of the secondary voltage rises to the no-load voltage condition, which due to the transformation ratio of the transformer can exceed the rated voltage.

Transmission line/cable: TOVs of power frequency occur after a load rejection at the receiving end of long transmission lines or cables because of their capacitive charge current, which leads to a negative voltage drop over the series impedances of the pi-equivalent circuit of the line or cable. Due to the Ferranti effect, the voltage at the open end of the line/cable will usually exceed the voltage at the sending end after load rejection.

Table 2 shows the steady state equations and the approximated voltage rise that occurs in each component after load rejection.

Component	Steady state equations	Voltage rise
Generator	$\underline{E}' \approx \underline{V}_G + jX'_d\underline{I}$ E' is the internal emf V_G is the terminal voltage X''_d is the *d*-axis subtransient reactance	$\Delta V = \left|\underline{V}_{G(o)}\right| - \left|\underline{V}_G\right|$ $\left|\underline{V}_{G(o)}\right| = \left|\underline{E}'\right|$ $\Delta V \approx \dfrac{X''_d Q_G}{V_G}$ $V_{G(o)}$ is the voltage at the secondary side after load rejection (i.e., with $I = 0$) Q_G is the reactive power supplied by the generator before load rejection
Transformer	$\underline{V}_P = t\left(\underline{V}_S + \underline{Z}_{sc}\underline{I}_S\right)$ $\underline{I}_P = \underline{I}_S / t$ V_P, V_S are the voltages at the primary and secondary side, respectively I_P, I_S are the currents at the primary and secondary side, respectively t is the transformation ratio, which is controlled by the transformer regulator Z_{sc} is the short-circuit impedance referred to the secondary side	$\Delta V = \left|\underline{V}_{S(o)}\right| - \left|\underline{V}_S\right|$ $\left|\underline{V}_{S(o)}\right| = \left|\dfrac{\underline{V}_P}{t}\right|$ $\Delta V \approx \dfrac{R_{sc}P_S + X_{sc}Q_S}{V_S}$ $V_{S(o)}$ is the voltage at the secondary side after load rejection (i.e., with $I_S = 0$) R_{sc}, X_{sc} are the short-circuit resistance and reactance, respectively P_S, Q_S are the active and reactive power at the secondary side before load rejection
Transmission line	$\begin{bmatrix} \underline{V}_S \\ \underline{I}_S \end{bmatrix} = \begin{bmatrix} \cosh\underline{\gamma}\ell & \underline{Z}_s\sinh\underline{\gamma}\ell \\ \underline{Y}_s\sinh\underline{\gamma}\ell & \cosh\underline{\gamma}\ell \end{bmatrix} \cdot \begin{bmatrix} \underline{V}_R \\ \underline{I}_R \end{bmatrix}$ $\underline{\gamma} = \alpha + j\beta = \sqrt{(R+j\omega L)(G+j\omega C)}$ $\underline{Z}_s = \sqrt{\dfrac{(R+j\omega L)}{(G+j\omega C)}} \quad \dfrac{1}{\underline{Y}_s} = \underline{Z}_s \quad \omega = 2\pi f$ V_S, V_R are the voltages at the sending and receiving end, respectively I_S, I_R are the currents at the sending and receiving end, respectively	$\Delta V = \left|\underline{V}_{R(o)}\right| - \left|\underline{V}_R\right|$ $\left|\underline{V}_{R(o)}\right| = \left|\dfrac{V_S}{\cosh\underline{\gamma}\ell}\right|$ $V_{R(o)}$ is the voltage at the receiving end after load rejection (i.e., with $I_R = 0$)

	γ is the propagation constant	
	Z_s is the surge impedance	
	R, L, G, C are the parameters per unit length	
	f is the power frequency	
	ℓ is the line length	

Table 2. Voltage rise at the power system components after load rejection

The equations of the table were derived by assuming that the load is disconnected at the terminals of the respective component. This is not the case of the system shown in Figure 5 since after load rejection at the receiving end of the transmission line, the no-load condition is strictly correct for the transmission line, but not for the transformer and the generator.

After load rejection the line remains under voltage and generating capacitive power; therefore the currents at the secondary side of the transformer and the generator terminals are not zero; in fact the currents for these two components can be large and capacitive, which will produce Ferranti effect and voltage rises larger than those obtained from the expressions given in the table.

Under such condition, the voltage rise at the generator and transformer terminals can be more accurately obtained by increasing the reactive power of the load with the capacitive power generated by the transmission line under no load condition. That is:

$$\Delta V \approx \frac{X_d''(Q_G + Q_\ell)}{V_G} \qquad \text{for the generator} \qquad (13a)$$

$$\Delta V \approx \frac{R_{sc}P_S + X_{sc}(Q_S + Q_\ell)}{V_S} \qquad \text{for the transformer} \qquad (13b)$$

where the reactive power generated by the line at its sending end when it is unloaded can be approximated by the following expression:

$$Q_\ell \approx V_S^2 \frac{\tan \gamma \ell}{Z_s} \qquad (14)$$

In the above equations, the subscripts G, ℓ, and S stand respectively for generator, line and sending end. Symbols used for variables and parameters are explained in Table 2. The value of the voltage at the sending end of the transmission line may significantly increase after load rejection since there can be a voltage rise at the secondary side of the transformer.

It is also important to consider the possibility that the reactive power at the generator terminals and the secondary side of the transformer is leading before load rejection; that

is, the reactive power generated by the transmission line (or cable) is larger or much larger that the reactive power of the load at the receiving end of the line (or cable).

4.3. Case Study

Figure 6 shows a 110-kV, 40-km line fed from a step-up transformer. The transformer is delta-wye connected with grounded neutral at the line side. The load at the end of the transmission line is 120 MVA, with a power factor of 0.87 (lagging). The entire load is suddenly disconnected by opening a switch at the receiving end of the line. Since the line is not too long and the voltage not too high, the Ferranti effect will not take place, so it should be assumed that there will not be voltage rise at the receiving end of the line with respect to its sending end. Plots of Figure 7 show the simulation results obtained when the generator exciter is included in the model.
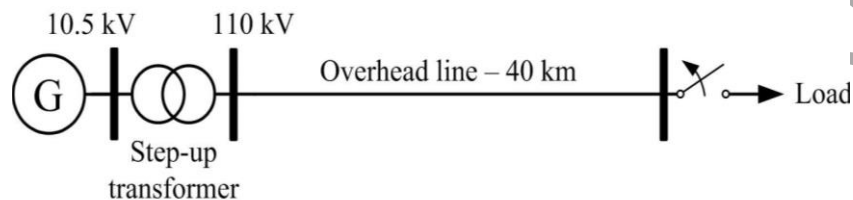
Figure 6. Load rejection. Diagram of the test system.

These results may be justified as follows. Since the generator exciter is included, the generator voltage comes back to its nominal value, and since the Ferranti effect is negligible, voltages at the transformer secondary and the receiving end of the line are basically the same once the load has been disconnected.

In this case the voltage rise at the remote end of the line is the result of several effects: the internal voltage drop in the transformer, which is almost negligible after load rejection, the voltage increase caused by the transformer ratio, which is working with a tap that produces a secondary voltage above the rated voltage (i.e., 110 kV) to compensate for the internal voltage drop, and the voltage drop along the line, which can be also assumed negligible.

Note, however, that although the steady state voltage rise at the remote end of the line above the rated voltage is not too high (about a 7%), the initial transient overvoltage reaches a value of 1.5 pu. It is also interesting to observe that the voltage rise in percentage of the initial voltage is more than 20%, since this initial voltage is below the 90% of the rated voltage as a consequence of the voltage drops in the transformer and the line.

Without the exciter model, there would be voltage rises at the generator terminals, at the secondary side of the transformer and at the remote end line terminals; consequently, the rise would be even higher and rather unrealistic.
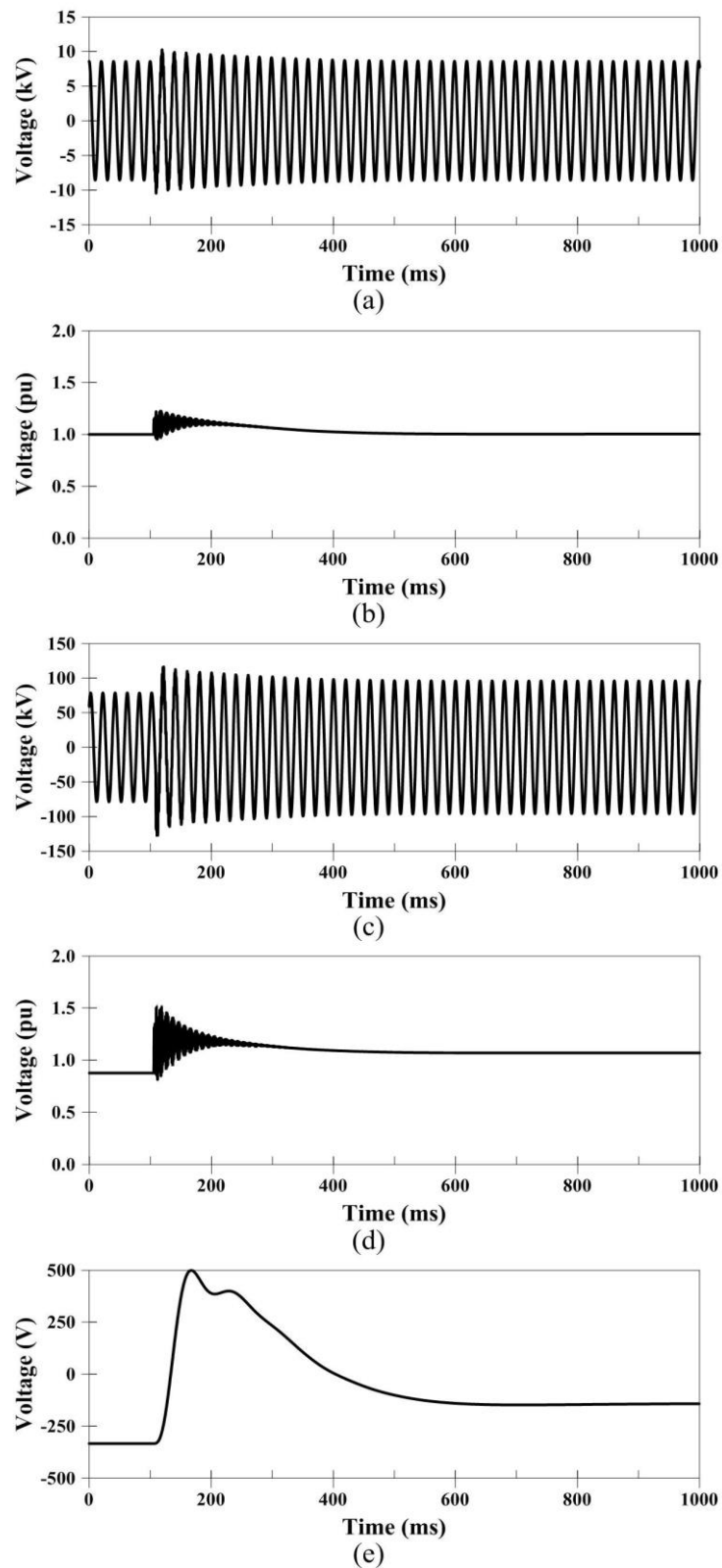
Figure 7. Load rejection study: Simulation results with control of generator excitation. (a) Voltage at generator terminal. (b) Rms voltage at generator terminal (in pu). (c) Voltage at the receiving end of the transmission line. (d) Rms voltage at the receiving end of the transmission line. (e) Generator exciter voltage.

4.4. Mitigation of Load Rejection Overvoltages

Overvoltages caused by load rejection can be controlled by shunt reactors, series capacitors or static compensators. The mechanism that leads to a reduction of the TOV can be justified by assuming that after compensation the new shunt reactance is composed of the original reactance X_C and a compensating shunt reactance X_{sh}; then, the effective capacitive reactance can be approached by:

$$X_{Cnew} \approx \frac{X_C}{1 - X_C / X_{sh}} \tag{15}$$

The effect of X_{sh} is to increase the effective reactance and to reduce the TOV.

Shunt reactors are placed at the ends of the line sections. They reduce transient overvoltages in the same way as TOVs. They can also provide the draining of trapped charges on isolated line sections which avoids excessive transient voltages when reclosing the line.

Shunt compensation may be seen as a reduction of the surge impedance, which can be a desirable condition in the initial phase of the system; i.e., when it operates with a light load. When the system is later operated at higher loads, the increased reactive demand of a line will cause an elevated excitation in the generators; this can have, on one hand, the favorable effect that the system becomes stiffer and exhibits a better performance with respect to stability, and, on the other hand, an unfavorable effect on both temporary and transient overvoltages, which will be higher.

The application of shunt compensation may take advantage of shunt reactors with a variable magnetizing characteristic; that is, to use saturation in a favorable way: once the point of increased magnetizing is exceeded then the reactor consumes an increased fundamental current component which effectively means augmented shunt compensation (Glavitsch, 1980). Obviously, reactors of this type produce harmonics which may act in an unfavorable way and even cause TOVs. According to Glavitsch (1980), the third harmonic plays a key role and consequently the zero-sequence system as seen from the location of the reactors. These reactors can be successfully applied to line lengths beyond 300 km. Below 300 km the third harmonic voltage is superimposed in an unfavorable way producing TOVs with a frequency of oscillation higher than the power frequency. However the absolute size of the voltages for these line lengths should be of no concern to the system planner. Load rejection overvoltages can be reduced from a level of 1.5 pu for linear reactors to a level of about 1.3 pu for gapped-core reactors.

When employing permanently connected reactors, reactive current has to be supplied during normal operation causing a reduction of the surge impedance loading, increased losses and an elevated excitation in the generators. This can be avoided by switching the reactors; i.e., connecting them when energizing the line and when shedding load. This can only be made to a limited extent because the switching operation during load shedding cannot be carried out fast enough. This may justify the use of reactors with an

extreme magnetizing characteristic; i.e., a negligible magnetizing current in the normal operating region and a rather flat characteristic above the rated flux (Glavitsch, 1980). Such reactor requires a special design to compensate the harmonics which make the equipment relatively expensive.

A more flexible compensation can be achieved by means of a static VAr compensator (SVC), in which thyristors are used control the reactive current through the inductance. The firing angle of two thyristors in an anti-parallel arrangement is used to control the current through the inductance, and determines the fundamental current which is a reactive current. The control range goes from zero to a maximum power of V^2/X, where V is the line voltage and X the reactance. Figure 8 shows a simplified diagram of this system arrangement.
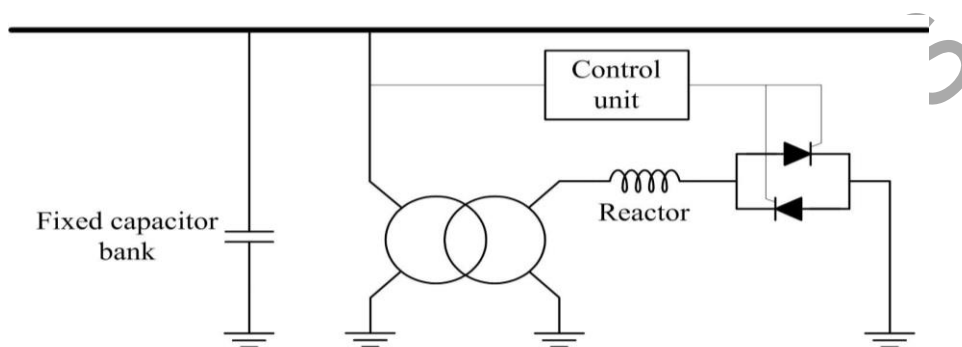
Figure 8. Single line diagram of a static VAr compensator.

The response of this compensation scheme is rather fast and only limited by the delays of the electronic regulator and the inherent time constant of the power circuit. A feasible response time is of the order of 10 ms, which means that for TOVs the effectiveness of this device is unquestionable, and it can be also considered for transient overvoltages. To take full advantage of the potential of reactive-power control, the compensator is usually complemented by capacitor banks to allow the supply of reactive power at a leading power factor to the system, see Figure 8. For reduction of TOVs, the decisive parameter is the inductance of the compensator. This compensation scheme can reduce reactive power during normal operation and quickly restore compensation in case of load rejection. Continuous control of reactive power is beneficial for the load flow, stability and the security of supply, which in certain cases may be the dominant aspect of controllable reactive compensation.

4.5. Conclusion

TOVs caused by load rejection are affected by the Ferranti effect in transmission lines. A very unfavorable condition is the load rejection of inductive reactive load. The sub-transient voltage step in a generator rises with a decreasing power factor, and rises with the rated power of the generator. Obviously, TOVs caused by partial load rejection with constant inductive reactive load are smaller than those caused by total load rejection.

Reactive compensation, either in the form of fixed shunt compensation or controllable compensation, is a common means to reduce these TOVs, and it can be supplemented

by appropriately structuring the system and by fast-acting voltage regulators in generators and transformers.

-

-

-

Bibliography

Adibi M.M., Alexander R.W., Avramovic B. (1992). Overvoltage control during restoration, *IEEE Trans. on Power Systems* 7, 1464-1470. [Comprehensive discussion of three related overvoltage areas -sustained power frequency overvoltages, switching transients, harmonic resonances- on the early stages of restoring high-voltage overhead and underground transmission lines].

Andrei R.G., Halley B.R. (1989). Voltage transformer ferroresonance from an energy transfer standpoint, *IEEE Trans. on Power Delivery* 4, 1773-1778. [This paper presents an approach to determine whether ferro-resonance can occur, and it is based on the energy transferred from the system to the voltage transformer during a switching transient].

Arturi C.M. (1991). Transient simulation and analysis of a three-phase five-limb step-up transformer following an out-of-phase synchronization, *IEEE Trans. on Power Delivery* 6, 196-207. [This paper presents theoretical and experimental analyses of electromagnetic transients following the out-of-phase synchronization of a three-phase five-leg step-up transformer].

Brunke J.H., Fröhlich K.J. (2001). Elimination of transformer inrush currents by controlled switching - Part I: Theoretical considerations, *IEEE Trans. on Power Delivery* 16, 276-280. [This paper explores the theoretical considerations of core flux transients, developing algorithms which allow controlled energization of most transformers without inrush current].

Brunke J.H., Fröhlich K.J. (2001). Elimination of transformer inrush currents by controlled switching - Part II: Application and performance considerations, *IEEE Trans. on Power Delivery* 16, 281-285. [This paper explores the practical considerations of core flux transients, performance of control strategies, and the application of circuit breakers to control transformer inrush transients].

Chen X. (2000). Negative inductance and numerical instability of the saturable transformer component in EMTP, *IEEE Trans. on Power Delivery* 15, 1199-1204. [This paper suggests a simple modification of the structure of the Saturable Transformer Component model, eliminating a typical numerical instability].

Cheng C.P., Chen S. (2006). Simulation of resonance over-voltage during energization of high voltage power network, *Electric Power Systems Research* 76, 650-654. [This paper describes the resonance overvoltages encountered during the energization of transformers in transmission systems, proposes the use of electromagnetic transient computer programs for resonance analysis, and suggests mitigation measures].

Cherry E.C. (1949). The duality between interlinked electric and magnetic circuits and the formation of transformer equivalent circuits, *Proc. of the Physical Society* 62, 101-111. [This paper presents the equivalent electric circuit of a transformer based on the topological principle of duality].

CIGRE WG 33.02 (1990). Guidelines for Representation of Network Elements when Calculating

Transients, CIGRE Brochure 39. [This brochure presents a review of guidelines proposed for representing power system components when calculating electromagnetic transients by means a computer].

Das J.C. (2002). *Power System Analysis. Short-Circuit, Load Flow and Harmonics*, New York, NY: Marcel Dekker. [This book presents theoretical and practical aspects of short-circuit analysis in power systems for computer-based studies that can be used in real-world applications].

Das J.C. (2010). *Transients in Electrical Systems. Analysis, Recognition, and Mitigation*, New York, NY: McGraw-Hill. [A practical and analytical guide for practicing engineers, and a reference book on transients in power systems].

de León F., Gómez P., Martinez-Velasco J.A., Rioual M. (2009). Transformers, Chapter 4 of *Power System Transients. Parameter Determination*, J.A. Martinez-Velasco (ed.), Boca Raton, FL: CRC Press. [This chapter details the type of transformer models to be used in transient analysis and simulation, and presents procedures for determining the parameters to be specified in those models].

de León F., Martinez J.A. (2009). Dual three-winding transformer equivalent circuit matching leakage measurements, *IEEE Trans. on Power Delivery* 24, 160- 168. [This paper presents an equivalent circuit for the leakage inductance of three-winding transformers based on the principle of duality, and matching terminal-leakage inductance measurements].

Dollan E.J., Gillies D.A., Kimbark E.W. (1972). Ferroresonance in a transformer switched with an EHV line, *IEEE Trans. on Power Apparatus and Systems* 91, 1273-1280. [This paper presents a discussion about the ferro-resonance phenomenon and its prevention on a bank of autotransformers].

Dommel H.W., (1992). *EMTP Theory Book*, 2nd Edition, Vancouver, BC, Canada: Microtran Power System Analysis Corporation. [This book is the reference text book for the Electromagnetic Transients Program].

Durbak D. (2006). Temporary overvoltages following transformer energizing, *Siemens PTI Newsletter* 99, 1-3. [This paper presents an introduction to the temporary overvoltages that can follow transformer energizing with emphasis on thise that occur during black start conditions].

EPRI Report (2005). Effects of Temporary Overvoltage on Residential Products: System Compatibility Research Project, Report 1008540, Palo Alto, CA. [This report presents an understanding of temporary overvoltages and the damage they can cause].

Ferracci P. (1998). Ferroresonance, Cahier Technique no. 190, Group Schneider. [This brochure presents a thorough study on the ferro-resonance phenomenon, predicting and evaluating its risk in existing and future installations, and also providing practical solutions designed to avoid or eliminate such phenomenon].

German D.M., Haddad A. (2004). Overvoltages and Insulation Coordination on Transmission Networks, Chapter 7 of *Advances in High Voltage Engineering*, A. Haddad and D. Warne (Eds.), Stevenage, UK: The Institution of Electrical Engineers. [This chapter presents a review of the origin of power system overvoltages, a discussion of the models to be used in their analysis and simulation, and a summary of insulation coordination procedures].

Germay N., Mastero S., Vroman J. (1978). Single phase ferroresonance on a 150/√3 kV voltage transformer: Comparison of measured and computer results, *Proc. of IEEE* 125, 533-535. [This paper presents a model for magnetic hysteresis which can be applied for reproducing the single-phase ferro-resonance phenomenon encountered in high voltage power systems].

Glavitsch H. (1980). Temporary Overvoltages, Chapter 7 in *Surges in High-Voltage Networks*, K. Ragaller (Ed.), 115-129, New York, NY: Plenum Press. [This chapter presents a description of temporary overvoltages and their origin, and details some of the most common methods for their compensation and damping].

POWER SYSTEM TRANSIENTS – *Temporary Overvoltages in Power Systems* - Juan A. Martinez-Velasco, Francisco González-Molina

Gole A., Martinez-Velasco J.A., Keri A. (eds.) (1998). Modeling and Analysis of Power System Transients Using Digital Programs, IEEE Special Publication TP-133-0, IEEE Catalog No. 99TP133-0. [This special publication presents an introduction to time-domain solution of electromagnetic transients in power systems using a digital computer. The publication covers two main topics: solution techniques and modeling of power components].

Hayashi T., Roberts D.P., Walve K., Östrup T. Degens A.J., Marconato R., Morin g., Ogawa t. Hatziargyriou N. (1990). Modeling and simulation of black start and restoration of an electric power system. Results of a questionnaire, *Electra* 131, 157-169. [This document presents the questionnaire proposed by the CIGRE WG 38.02 to collect information about problems to be considered, studies to be carried out, and tools to be used for black start analysis].

Henriksen T. (2002). How to avoid unstable time domain responses caused by transformer models, *IEEE Trans. on Power Delivery* 17, 516-522. [This paper provides a solution for the unstable condition found typically in modeling three-winding transformers].

Hileman A.R. (1999). *Insulation Coordination for Power Systems*, New York, NY: Marcel Dekker. [A detailed and comprehensive reference book for power system insulation coordination].

Hopkinson R.H. (1965). Ferroresonance during single-phase switching of 3-phase distribution transformer banks, *IEEE Trans. on Power apparatus and Systems* 84, 289-293. [This paper uses transient network analyzer studies to determine the necessary conditions for the occurrence of resonance during single-phase switching of distribution transformer banks].

IEC 60071-1 (2010). Insulation Co-ordination, Part 1: Definitions, principles and rules. [This standard specifies the procedure for the selection of the rated withstand voltages for the phase-to-earth, phase-to-phase and longitudinal insulation of the equipment and the installations of these systems].

IEC 60071-2 (1996). Insulation co-ordination, Part 2: Application guide. [This standard provides guidance for the determination of the rated withstand voltages for ranges I and II of IEC 60071-1 and justifies the association of these rated values with the standardized highest voltages for equipment; it covers phase-to-phase, phase-to-earth and longitudinal insulation of three-phase systems with nominal voltages above 1kV].

IEC 60099-5 (2000). Surge arresters - Part 5: Selection and application recommendations, Edition 1.1. [This standard provides recommendations for the selection and application of surge arresters to be used in three-phase systems with nominal voltages above 1kV].

IEC TR 60071-4 (2004). Insulation Co-ordination - Part 4: Computational Guide to Insulation Co-ordination and Modelling of Electrical Networks. [This technical report provides guidance on conducting insulation co-ordination studies which propose internationally recognized recommendations for the implementation of deterministic and probabilistic methods adapted to the use of numerical programs].

IEEE Std C62.22 (1997). IEEE guide for the application of metal-oxide surge arresters for alternating-current systems. [This standard covers the application of metal-oxide surge arresters to safeguard electric power equipment against the hazards of abnormally high voltage surges of various origins].

IEEE Std C62.82.1 (2010). IEEE Standard for Insulation Coordination – Definitions, Principles and Rules. [This standard provides the procedure for selection of the withstand voltages for equipment phase-to-ground and phase-to-phase insulation systems].

IEEE Std 1313.2 (1999). IEEE Guide for the Application of Insulation Coordination. [This standard provides the calculation method for selection of phase-to-ground and phase-to-phase insulation withstand voltages for equipment].

Iravani R., Chaudhury A.K.S., Hassan I.D., Martinez J.A., Morched A.S., Mork B.A., Parniani M., Shirmohammadi D., Walling R.A. (1998). Modeling Guidelines for Low Frequency Transients, Chapter 3 of *Modeling and Analysis of System Transients Using Digital Programs*, A. Gole, J.A. Martinez-Velasco

and A. Keri (eds.), IEEE Special Publication TP-133-0, IEEE Catalog No. 99TP133-0. [This report provides a brief explanation of the most common low-frequency transients in power systems, suggests modeling guidelines for time-domain simulation and analysis, and presents some typical test systems and simulation results].

Iravani M.R., Chaudhary A.K.S., Giewbrecht W.J., Hassan I.E., Keri A.J.F., Lee K.C., Martinez J.A., Morched A.S., Mork B.A., Parniani M., Sarshar A., Shirmohammadi D., Walling R.A., Woodford D.A. (2000). Modeling and analysis guidelines for slow transients: Part III: The study of ferroresonance, *IEEE Trans. on Power Delivery* 15, 255-265. [This paper introduces the ferro-resonance phenomenon and provides a general modeling approach].

Jacobson D.A.N., Swatek D., Mazur R. (1996). Mitigating potential transformer ferroresonance in a 230 kV converter station, *IEEE T&D Conference*, Los Angeles. [This paper presents a new tool, the two-dimensional bifurcation diagram, for visualizing the ferro-resonance phenomenon on a real case, the failure of a wound potential transformer that failed catastrophically on the Manitoba Hydro system].

Ketabi A., Ranjbar A.M., Feuillet R. (2002). Analysis and control of temporary overvoltages for automated restoration planning, *IEEE Trans. on Power Delivery* 17, 1121-1127. [This paper presents a new approach that assists power system restoration planning with regards to control of temporary overvoltages due to transformer energization].

Kieny C. (1991). Application of the bifurcation theory in studying and understanding the global behavior of a ferroresonant electric power circuit, *IEEE Trans. on Power Delivery* 6, 866-872. [This paper presents a permanent nonperiodic case of the ferro-resonance phenomenon observed on a 400 kV power system].

Leonardo Report (2008). Transient and Temporary Overvoltages and Currents-Annex D: Ferroresonance Effects, *Power Quality and Utilisation Guide*. [This report presents a review on the ferro-resonance phenomenon].

Lindenmeyer D., Dommel H.W., Moshref A., Kundur P. (1999). Analyis and control of harmonic overvoltages during system restoration, *Int. Conf. on Power Systems Transients* (*IPST*), Budapest. [This paper presents a new method which facilitates power system restoration planning with respect to the control of harmonic resonance overvoltages].

Martinez J.A., Mork B. (2005). Transformer modeling for low- and mid-frequency transients - A review, *IEEE Trans. on Power Delivery* 20, 1625-1632. [This paper reviews transformer models for simulation of low- and mid-frequency transients].

Martinez J.A., Walling R., Mork B., Martin-Arnedo J., Durbak D. (2005). Parameter determination for modeling systems transients. Part III: Transformers, *IEEE Trans. on Power Delivery* 20, 2051-2062. [This paper provides guidelines for the estimation of parameters to be specified when simulating low- and mid-frequency transient phenomena].

Morin G. (1987). Service restoration following a major failure on the Hydro-Quebec power system, *IEEE Trans. on Power Delivery* 2, 454-463. [This paper presents an approach to service restoration which should speed up the process of restoring service to customers].

Mork B.A., Stuehm D.L. (1994). Application of nonlinear dynamics and chaos to ferroresonance in distribution systems, *IEEE Trans. on Power Systems* 9, 1009-1017: [This paper identifies a ferro-resonant circuit as a nonlinear dynamical system, and presents methods providing new insights into the global behavior of ferro-resonance].

Mork B.A. (1999). Five-legged wound-core transformer model: Derivation, parameters, implementation, and evaluation, *IEEE Trans. on Power Delivery* 14, 1519-1526. [This paper presents an equivalent circuit, derived using duality transformations, for the widely used three-phase grounded-wye to grounded-wye five-legged wound-core distribution transformer].

Mork B.A., Gonzalez F., Ishchenko D., Stuehm D.L., Mitra J. (2007). Hybrid transformer model for transient simulation: Part I: Development and parameters, *IEEE Trans. on Power Delivery* 22, 248-255. [This paper presents a new topologically correct hybrid transformer model for low- and mid-frequency transient simulations].

Povh D., Schultz W. (1978). Analysis of overvoltages caused by transformer magnetizing inrush current, *IEEE Trans. on Power Apparatus and Systems* 97, 1355-1365. [This paper provides a comprehensive discussion about systems with pronounced resonance conditions and a low degree of damping, where temporary overvoltages may develop when transformers are switched in or at fault clearing].

Slemon G.R. (1953). Equivalent circuits for transformers and machines including non-linear effects, *Proc. IEE* 100, 129-143. [This paper proposes simple equivalent circuits for transformers and rotating machines].

Stuehm D.L., Mork B.A., Mairs D.D. (1989). Five-legged core transformer equivalent circuit, *IEEE Trans. on Power Delivery* 4, 1786-1793. [This paper presents a three-phase equivalent circuit model for five-legged core grounded-wye-to-grounded-wye transformers].
Sybille G., Gavrilovic M.M., Belanger J., Do V.Q. (1985). Transformer saturation effects on EHV system overvoltages, *IEEE Trans. on Power Apparatus and Systems* 104, 671-680. [This paper presents an analysis on effects such transformer energization, fault application and clearing, and load rejection].

Van Craenenbroeck T., Van Dommelen D., Janssens N. (2000). Damping circuit design for ferroresonance in floating power systems, *European Transactions on Electrical Power* 10, 155-159. [This paper presents practical countermeasures in order to prevent the occurrence of ferro-resonance in floating systems].

Walling R.A., Barker K.D., Compton T.M., Zimmerman I.E. (1993). Ferroresonant overvoltages in grounded padmount transformers with low-loss silicon-steel cores, *IEEE Trans. on Power Delivery* 8, 1647-1660. [This paper presents the results of an extensive test program, applied on a grounded wye-wye three-phase distribution transformers using a five-leg silicon steel wound core, in order to study the ferro-resonance phenomenon].

Biographical Sketches

Juan A. Martinez-Velasco was born in Barcelona (Spain). He received the Ingeniero Industrial and Doctor Ingeniero Industrial degrees from the Universitat Politècnica de Catalunya (UPC), Spain. He is currently with the Departament d'Enginyeria Elèctrica of the UPC. His teaching and research areas cover Power Systems Analysis, Transmission and Distribution, Power Quality and Electromagnetic Transients. He is an active member of several IEEE and CIGRE Working Groups. Presently, he is the chair of the IEEE WG on Modeling and Analysis of System Transients Using Digital Programs.

Francisco Gonzalez was born in Barcelona (Spain). He received the M.S. and Ph.D. degrees from Universitat Politecnica de Catalunya (Spain), in 1996 and 2001. As a Visiting Researcher, he worked with the Norwegian Institute of Science and Technology (Norway), Tennessee Technological University (USA), North Dakota State University (USA), and Michigan Technological University (USA), the latest one under a Postdoctoral Fellowship awarded by the Spanish Government. His experience also includes five years working as Corporate Business Development Director in El Sewedy Cables (Egypt), one of the biggest electrical material manufacturers worldwide. Nowadays, Dr. Gonzalez works as Assistant Professor in the Dept. of Electrical Engineering at the Universitat Rovira i Virgili (Spain). His research interests include transient analysis of power systems, lightning performance of transmission and distribution lines, power quality, and renewables.